

Active Power Filtering Implementation Using Photovoltaic System with Reduced Energy Storage Capacitor

Horng-Yuan Wu, Chin-Yuan Hsu, Tsair-Fwu Lee*, *Member, IEEE.*

Abstract—A novel three-phase active power filter (APF) circuit with photovoltaic (PV) system to improve the quality of service and to reduce the capacity of energy storage capacitor is presented. The energy balance concept and sampling technique were used to simplify the calculation algorithm for the required utility source current and to control the voltage of the energy storage capacitor. The feasibility was verified by using the Pspice simulations and experiments. When the APF mode was used during non-operational period, not only the utilization rate, power factor and power quality could be improved, but also the capacity of energy storage capacitor could sparing. As the results, the advantages of the APF circuit are simplicity of control circuits, low cost, and good transient response.

Keywords—active power filter, sampling, energy-storage capacitor, harmonic current, energy balance.

I. INTRODUCTION

POWER electronics circuits are widely used in many different types of industrial equipment, such as frequency changers, motor drive systems, etc. This equipment presents nonlinear impedance to the utility, generating large harmonic currents with well known negative effects, such as a low power factor, low efficiency and destruction of other equipment (e.g. the power capacitor can be damaged by the resonant over-voltage etc.). Also, some precision instruments and communication equipment will be interfered with the electromagnetic interference (EMI). Therefore, utility power quality has become an important issue recently. Many research papers and methods have been proposed to solve these problems. Conventionally, a passive L-C filter was used to suppress the harmonics. Capacitors were used to compensate the lag power factor. However, they have many disadvantages, such as large size, resonance, and fixed compensation characteristics [1, 2]. Therefore, conventional passive power filter can not provide a complete solution.

Many specialists approach the solution from the viewpoint of preventing the generation of harmonics, such as high power factor switching power supply, frequency changer and

uninterruptible power supply (UPS) etc. [3-7] However, the present harmonic pollution sources, still need to be improved. Some APF methods have been proposed to compensate for the present harmonic loads. They are in the type of parallel with the non-linear load to provide the reactive power and to compensate for the harmonic current, in order to achieve the goal of high quality of service of utility sources [8-14].

Due to the limitations of sunshine, the average operating time of a PV system is only 6–8 hours. Hence, the equipment of a PV system operates at a low utilization rate. If the system is transferred to the APF operation mode during non-operational moments, so that the utilization rate, power factor and power quality can be improved [15].

This paper proposes a new three-phase active power filter (APF) technique, based on the concept of energy balance. At the end of each period, we use a sampling technique to detect the energy deviation of the energy-storage capacitor and to calculate the peak value of utility command current at the end of each period. By employing a set of a three-phase sinusoidal reference voltage in phase with the utility source to multiply with this peak value, we can obtain the required utility source current. The difference between the instantaneous load current and this current is the command current for the APF. This command current includes reactive fundamental power and harmonics. The current is provided by a bilateral converter using a hysteresis current control technique [16-20].

Because the instantaneous fundamental reactive power of a balanced three-phase system is zero, the instantaneous fundamental reactive power transfers only among phases. In theory, the required capacity of the energy-storage capacitor is zero. But, harmonics power transfers between the load and the energy-storage capacitor (charging and discharging), hence we still need to use a small capacitance for the energy-storage, and the average capacitor voltage can be maintained at a constant value. However, due to the losses in the converter such as switching loss, capacitor leakage current etc., the utility must provide not only the real power needed by the load but also these overhead required by converter to maintain the capacitor voltage at a prescribed value.

In this paper, a new DC bus voltage controller, using the energy balance concept, is proposed. As there is no delay element (such as LPF or PI control) used in this control circuit, and the transient response is fast and good.

H.-Y. Wu and C.-Y. Hsu are with the Department of Electrical Engineering, National Kaohsiung University of Applied Sciences. (E-mail: thywu@mail.ee.kuas.edu.tw).

T.-F. Lee is with the Department of Electronic Engineering, National Kaohsiung University of Applied Sciences. (*Corresponding author, phone: 886-7-3814526; fax: 886-7-3811182; E-mail: tflee@byte.ec.kuas.edu.tw).

II. PRINCIPLES OF OPERATION

A. System description

The basic circuit configuration of a utility interactive PV system is shown in Fig.1. The battery bank of a DC bus is replaced by a capacitor due to less power storage in the DC bus. The system configuration is the same as APF except for the DC converter stage. DC converter stage will be disabled and the system will be transferred to APF mode during non-operation duration. The Fig. 1(a) shows the utility interaction PV system operates on generation mode, and the Fig. 1(b) shows the system operates on APF mode.

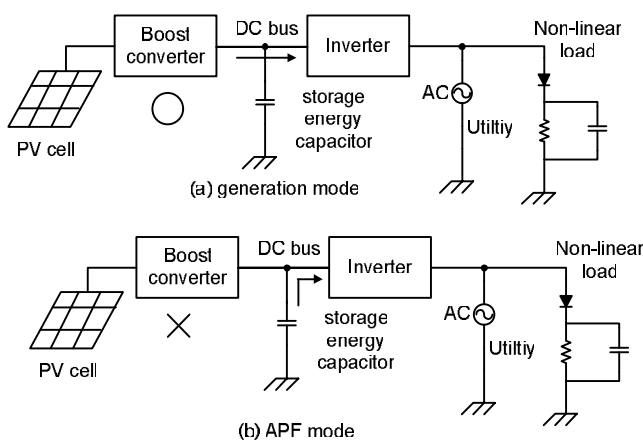


Fig. 1 The block diagram of PV power supply system

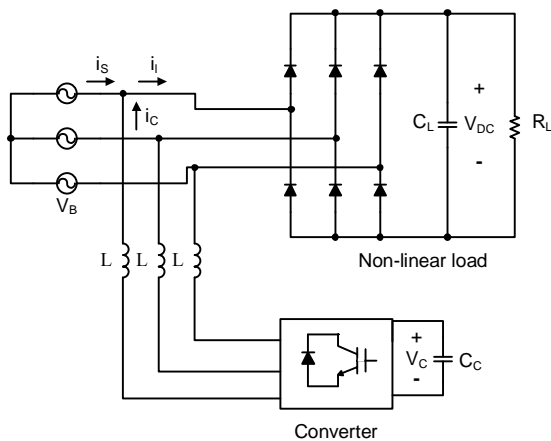


Fig. 2 The block diagram of the three-phase APF system

The fundamental building block of the three-phase APF system is shown in Fig.2. Under normal circumstances, the utility can be assumed as a sinusoidal voltage source.

$$v_{s,k}(t) = V_{sm} \operatorname{Re} e^{j(\omega t - k \frac{2\pi}{3})}, \quad k = -1, 0, \text{ and } 1 \quad (1)$$

If a nonlinear load is applied, then the load current will consist of the fundamental component and all the higher order harmonics. It can be represented as

$$i_{l,k}(t) = \sum_{n=1}^{\infty} I_{l,n} \operatorname{Re} e^{j(n(\omega t - k \frac{2\pi}{3}) + \theta_n)}, \quad k = -1, 0, \text{ and } 1 \quad (2)$$

Therefore, the three-load power can be expressed as

$$\begin{aligned} p_{total,l}(t) &= \sum_{k=-1}^1 v_{s,k}(t) \times i_{l,k}(t) \\ &= \frac{3}{2} V_{sm} I_{l,1} \cos \theta_1 + \frac{1}{2} \sum_{k=-1}^1 V_{sm} I_{l,1} \operatorname{Re} e^{j(2\omega t - k \frac{4\pi}{3} + \theta_1)} \\ &\quad + V_{sm} \sum_{k=-1}^1 \sum_{n=2}^{\infty} I_{l,n} \operatorname{Re} e^{j(\omega t - k \frac{2\pi}{3})} \operatorname{Re} e^{j(n(\omega t - k \frac{2\pi}{3}) + \theta_n)}, \end{aligned} \quad (3)$$

where $k = -1, 0, \text{ and } 1$

In eq.(3), the first term is the real power supplied by the utility source, the second term is the reactive power, and the third term is the harmonic power. The last two terms are supplied by the APF. For a balanced three phase system, the second term is zero, i.e.

$$p_{total,l}(t) = P_s + p_{total,c}(t) \quad (4)$$

$$P_s = \frac{3}{2} V_{sm} I_{l,1} \cos \theta_1 = \frac{3V_{sm} I_m}{2} \quad (5)$$

$$p_{total,c}(t) = V_{sm} \sum_{k=-1}^1 \sum_{n=2}^{\infty} I_{l,n} \operatorname{Re} e^{j(\omega t - k \frac{2\pi}{3})} \operatorname{Re} e^{j(n(\omega t - k \frac{2\pi}{3}) + \theta_n)}, \quad (6)$$

where $k = -1, 0, \text{ and } 1$

As the APF provides the harmonic power $P_{total,c}$, the current supplied by the utility will be

$$i_{s,k}(t) = I_m \operatorname{Re} e^{j(\omega t - k \frac{2\pi}{3})} \quad (7)$$

where

$$I_m = \frac{2P_s}{3V_{sm}} = I_{l,1} \cos \theta_1 \quad (8)$$

The current $i_{s,k}(t)$ is in phase with the utility voltage and is pure sinusoidal. Therefore, The APF must provide the compensation current.

$$i_{c,k}(t) = i_{l,k}(t) - i_{s,k}(t) \quad (9)$$

Hence, the APF needs to calculate the current $i_{s,k}(t)$ accurately and instantaneously as described in the following.

B. Calculation of fundamental component $i_{s,k}(t)$

For a three-phase APF in a steady state, the energy transformations are shown in Fig. 3.

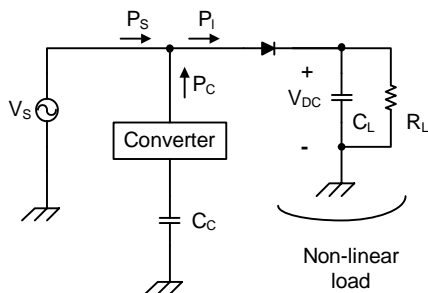


Fig. 3 The energy transfers in APF

The power consumption of the load is

$$P_L = \frac{V_{DC}^2}{R_L} \tag{10}$$

This power will be provided by the utility source. Because the reactive power and harmonic power are supplied by APF, the utility only needs to supply the pure sinusoidal current and in phase with the utility voltage (i.e. $pf=1.0$). The power supplied by the utility is

$$P_s = \frac{3V_{sm}I_m}{2} \tag{11}$$

where

$$I_m = \frac{V_{DC}^2}{R_L} \cdot \frac{2}{3V_{sm}} \tag{12}$$

In theory, the energy-storage capacitor does not need to provide real power to the load. Therefore, at the end of one complete utility cycle, the terminal voltage of storage energy capacitor of converter will keep no change. However, owing to the switching loss and conductive loss of the power converter, the utility must provide not only the real power needed by the load (i.e. the in phase pure sinusoidal current $i_{s,k}(t)$), but also the additional power required by the converter to maintain the capacitor voltage at the prescribed value.

The change of energy-storage capacitor in one period will be

$$\Delta E_c = \frac{1}{2} C_c (V_{ref}^2 - V_c^2) \tag{13}$$

where

V_{ref}^2 the reference voltage of the energy-storage capacitor in steady state

V_c^2 the voltage of the energy-storage capacitor at the end of each utility period.

If the energy loss of the capacitor can be compensated to the set value desired at the end of the next utility cycle by the extra utility current $\Delta I_m \sin \omega t$, then in this cycle the energy compensated by the utility will be

$$\Delta E_c = \frac{3}{T} \int_0^T (V_{sm} \sin \omega t \times \Delta I_m \sin \omega t) dt = \frac{3V_{sm}\Delta I_m}{2} \times T \tag{14}$$

Based on the concept of energy balance, the compensation energy from the utility must equal to the energy loss of the energy-storage capacitor, i.e. $\Delta E_s = \Delta E_c$. Therefore, in the next period the variation of the utility current is

$$\Delta I_m = \frac{C_c (V_{ref}^2 - V_c^2)}{3V_{sm}T} = K (V_{ref}^2 - V_c^2) \tag{15}$$

where $K = \frac{C_c}{3V_{sm}T}$

Keep in mind, this energy-loss is caused by the increment of load. If the utility makes only this variation of current, ΔI_m , it will just keep the capacitor voltage from not dropping again, and be unable to pull the capacitor voltage back to the reference level. For the capacitor voltage to return to its reference value V_{ref} at the end of the next cycle, the utility must provide $2\Delta I_m$ current variation in the next cycle (one ΔI_m is for the load increment and other ΔI_m is for the compensation of energy loss in the previous cycle).

Figure 4 shows the control block diagram of energy-storage capacitor voltage. The input is the terminal voltage of the capacitor. It follows an attenuation circuit (K_1) to adjust this voltage to an appropriate level (V_c/K_1). Then, it is connected to an isolation amplifier to isolate the main power circuit from the control circuit. The value of V_c^2 is calculated by a square circuit. The other input is the reference voltage (V_{ref}/K_1), it also follows a square circuit to calculate V_{ref}^2 . The difference between $(V_c/K_1)^2$ and the set value $(V_{ref}/K_1)^2$ is multiplied by K_2 ($K_2 = K_1^2 \times K$) to get ΔI_m . This current ΔI_m adds to the previous command current I_{UP1} to obtain the steady-state utility command current of this coming period, I_{UP} . At the same time, one more ΔI_m adds to the steady-state utility command current I_{UP} , to get I_m ($I_m = I_{UP} + \Delta I_m$), and it will include the component to compensate the energy loss of the previous period. At the end of this coming period, the terminal voltage of energy-storage capacitor will return to V_{ref} .

These values are sampled at the end of each period by the sample and hold the circuit to keep the value until the end of next period. Hence, during each period, the change of energy-storage capacitor voltage does not affect the compensation characteristics of the APF. That means the capacitor can endure a much larger voltage ripple. As the results, we can reduce the capacity of this capacitor.

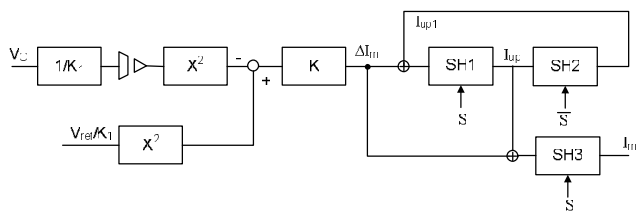


Fig. 4 The control block diagram of energy-storage capacitor voltage

C. The current tracking circuit

The block diagram of current tracking and control circuit are shown in Fig. 5. The voltage of phase A, $v_A(t)$, is connected to a zero cross detecting circuit (ZCD) to get a synchronous reference square wave. It will be used as the input of the phase lock loop (PLL). Using the PLL technique, we can get 256 times of the frequency of the utility source and the most significant bit of the frequency divider (Q_7) which is synchronous with the utility source. The output of frequency divider of PLL ($Q_0 \sim Q_7$) is used as the phase inputs of the three-phase sinusoidal reference voltage generator. The value of I_m is used as the reference voltage of the multiplier type digital to analog converter (DAC) to generate the utility command current i_s^* .

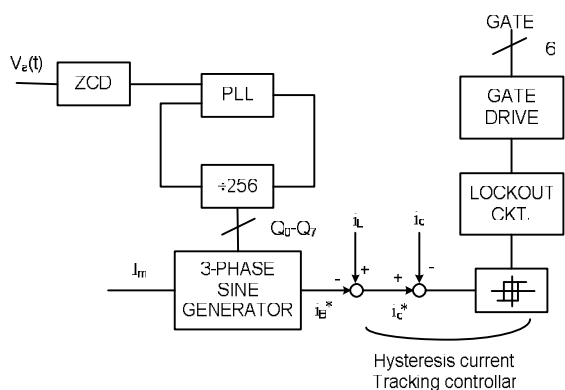


Fig. 5 The block diagram of current tracking and control circuit

We subtract the utility command current i_s^* from the load current i_L to get the compensation command current of the APF, i_c^* . This is used as the input signal for the three sets of hysteresis-type current tracking circuits which control the power switching devices (Insulated Gate Bipolar Transistor, IGBT) to generate a precise compensation current for each phase. The compensation current for each phase can compensate the utility current to be purely sinusoidal with unit power factor.

The three-phase sinusoidal reference waveform is generated by a look-up table (which was stored in an EPROM), as shown in Fig.6. The three-phase sinusoidal waveform data are pre-programmed in EPROM and read out sequentially according to the phase input $Q_0 \sim Q_7$. Then we use a multiplier

type digital to analog converter (DAC) to convert these binary data to a set of three-phase sinusoidal reference voltage data.

The reference voltage of DAC is directly fed from the command current I_m of the capacitor voltage control circuit. We can omit two sets of multipliers and directly generate the three-phase sinusoidal command current i_s^* by using a multiplier type DAC. This is the reason for using the multiplier type DAC.

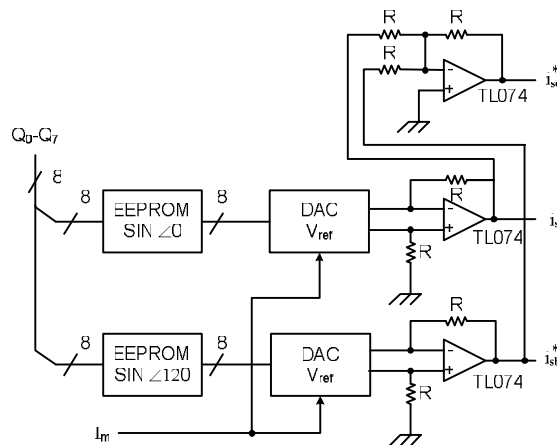


Fig. 6 The block diagram for generating three phase sinusoidal reference waveform

D. Improvement of the transient response

In a balanced three-phase system, the summation of three-phase instantaneous reactive power is zero, which means the reactive power transfers only among phases. In the steady state, the energy-storage capacitor is not the same as the single-phase APF capacitor that must be provide large reactive power (reactive power transfers between load and converter). Therefore the energy-storage capacitor of three-phase APF can take a small size capacitor to operate. However, in practical experimental circuits, we use a 22μf capacitor for compensating the unbalance of line voltage, the unbalance of the load impedance and also the harmonic power. The test results show that under the condition of 2A load current, it has good compensation characteristics.

But, in the transient state, due to the command current of APF is calculated according to the utility current in a previous period, the extra current in current period will be supplied from the energy-storage capacitor. Using a smaller size of energy-storage capacitor, the loss of energy will make the terminal voltage of the energy-storage capacitor discharge rapidly. The capacitor voltage may drop to below the peak valve of the rectified utility ($V_{C-limit}$), as shown in Fig.7. For example, when the load changes at t_1 (increasing load current), the capacitor voltage will discharge down to under the value of $V_{C-limit}$. However, because the anti-paralleled diode of the power switching device (IGBT or power MOSFET), the capacitor voltage can not drop down to under the value of $V_{C-limit} = \sqrt{2}V_{L-L}$. The voltage will keep at

$\sqrt{2}V_{L-L}$ until the start of next period, Since the value of ΔV_C , that is used for calculating the command current of the next period, is not in linear region (which shall be $\Delta V_C'$), the variation of the utility current ΔI_m , that is calculated with eq.(15), is not correct. Hence it can not recharge the capacitor back to V_{ref} at the end of the new period. Therefore, in the transient state, the control circuit must be modified.

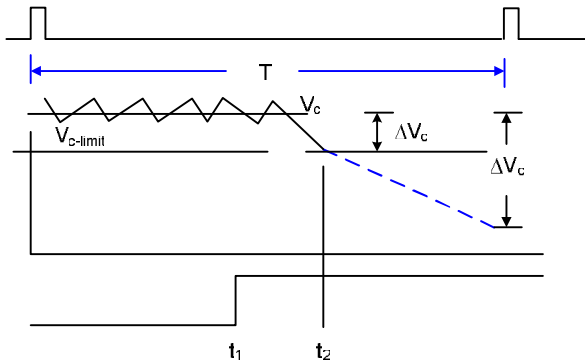


Fig. 7 The voltage of energy-storage capacitor under the transient state (load change at t_1)

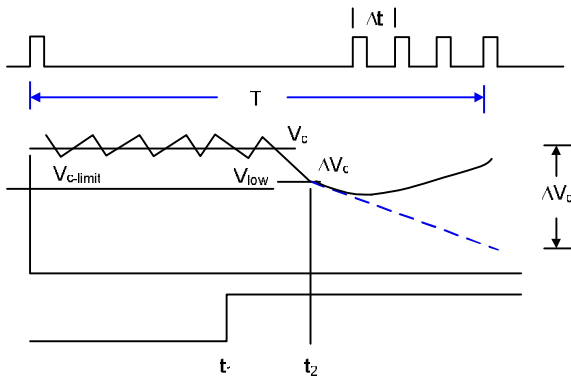


Fig. 8. The voltage of energy-storage capacitor under the transient state (using advanced sampling technique)

For example, in the case of the increase of load current is as shown in Fig. 8, the load current changes at t_1 , and the charging current $i_s(t)$ is smaller than the load current. The voltage V_C drops down. At t_2 , when the V_C is equal to V_{low} , we begin to modify the utility command current in advance. Under this new loading state, the changes of the utility command current are analyzed as follows:

The energy loss of the capacitor until t_2 is

$$\Delta E_c' = \frac{1}{2} C_c (V_{ref}^2 - V_{low}^2) \quad (16)$$

If we wish to recover the capacitor voltage to V_{ref} during the remaining time in this period, the utility command current must be increased by an amount of

$$\Delta I_m = \frac{C_c (V_{ref}^2 - V_c^2) T}{(t_2 - t_1) 3V_{sm} (T - t_2)} = K' (V_{ref}^2 - V_c^2) \quad (17)$$

where

$$K' = \frac{KT^2}{(t_2 - t_1)(T - t_2)} \quad (18)$$

Since the modified value of K' changes according to t_1 and t_2 , it is difficult to implement in the hardware. If I_m is updated immediately, using the K' in eq.(18), it will be often too large and will push the control system into saturation. Furthermore, the capacitor voltage cannot drop down to under the value of $V_{C-limit}$, hence we cannot accurately calculate the utility increment current directly from the capacitor voltage.

In practice, when the capacitor voltage drops down to below V_{low} , the controller sends out the sampling signal for updating the utility command current, using original K in order to increase the utility current. Although, this current is smaller than the real need for the new load current, it can decrease the drop-down speed of the capacitor voltage. If the new I_m is updated at the rate of Δt , this is equivalent to increasing the utility command current by ΔI_m at every update time. Therefore, after n sampling pulses, it is equivalent to increasing the utility command current by $n \times \Delta I_m$.

Eventually, the utility command current will be able to provide the energy needed for the new loading current. The capacitor voltage will be charged up from $V_{C-limit}$ and return to the linear region again. Then the amount ΔI_m decays progressively and the capacitor voltage will approach to V_{ref} . After the capacitor voltage rises over V_{low} , the system will be stayed in the linear region and the APF can work in steady-state during the next new period.

E. Determination of energy-storage capacitor

When the voltage or the load of a three-phase system is in an unbalanced condition, the instantaneous summation of the line frequency volt-ampere supplied from the energy-storage capacitor is not equal to zero. Assuming that under the steady state condition, the volt-ampere which needs to be compensated is equal to S_{UB} , then the maximum energy supplied by the capacitor will be equal to

$$\Delta E_{UB,max} = S_{UB} \times \frac{T}{2} \quad (19)$$

If this energy output make the capacitor voltage drop down to V_{low} , (i.e. $V_{C-limit} + 0.2(V_{ref} - V_{C-limit})$), then

$$\Delta E_{UB,max} = \frac{1}{2} C_{C,UB} (V_{ref}^2 - V_{low}^2) \quad (20)$$

$$C_{C,UB} = \frac{S_{UB} \cdot T}{(V_{ref}^2 - V_{low}^2)} \quad (21)$$

For example, if $V_{L-L} = 220V$, $S = 10 \text{ kVA}$, $S_{UB} = 10\% \times S = 1.0 \text{ kVA}$, $V_{C-limit} = 311V$, $V_{ref} = 1.5 V_{C-limit}$, and $V_{low} = 1.1 V_{C-limit}$, then $C_{C,UB} = 165\mu\text{f}$, i.e., $6.25\mu\text{f}/\text{amp}$.

On the other hand, the power absorbed by the nonlinear load can be represented as [17]

$$p_L(t) = \sum_{k=1}^1 v_{s,k}(t) \cdot \sum_{k=1}^1 i_{L,k}(t) = P_L + \tilde{p}(t) \quad (22)$$

with

$$P_L = \frac{3V_{sm} \cdot I_{L1} \cos \phi_1}{2} \quad (23)$$

P_L is the DC component relating to the real power consumed by the load.

$$\tilde{p}_L(t) = \sum_{n=1}^{\infty} P_{3n} \cos(3n\omega t - \varphi_{3n}) \quad (24)$$

For the six-pulse rectified load, the above equation will be expressed as

$$\tilde{p}_L(t) = \sum_{n=1}^{\infty} P_{6n} \cos(6n\omega t - \varphi_{6n}) \quad (25)$$

In this equation, the six-order harmonic will be the largest, and this six-order harmonic energy supplied by the capacitor will be

$$P_{6,L} \cdot \frac{T}{12} = \frac{1}{2} C_{C,HR} (V_{ref}^2 - V_{low}^2) \quad (26)$$

i.e.

$$C_{C,HR} = \frac{T \cdot P_{6,L}}{6(V_{ref}^2 - V_{low}^2)} \quad (27)$$

As in the previous case, if we assume $P_{6,L} = \frac{P_L}{2}$, then $C_{C,HR} = 132\mu\text{f}$ ($6\mu\text{f}/\text{amp}$). If we consider the both cases simultaneously, then the capacitor value is suggested as.

$$C_C = \sqrt{C_{C,UB}^2 + C_{C,HR}^2} \quad (28)$$

F. Determination of the advanced sampling time interval Δt

Assuming the maximum allowed transient current of this control system to be $\Delta I_m''$, at this time t_2 , the capacitor voltage drops down to the value of $V_{C-limit}$. Therefore the control system will modify the utility command current, using the advanced sampling technique. Since the capacitor voltage already drops down to the value of $V_{C-limit}$, the updated amount, $\Delta I_m'$, for each sampling is constant. In the time duration of $T-t_2$, the total advanced modified amount of the utility command current will be

$$\Delta I_m' + \Delta I_m' + \dots + \Delta I_m' = \Delta I_m'' \quad (29)$$

$$n = \frac{\Delta I_m''}{\Delta I_m'}$$

where

$$\Delta I_m' = K(V_{ref}^2 - V_{c,limit}^2) \quad (30)$$

Hence Δt will be determined as.

$$\Delta t = \frac{T - t_2}{n} \quad (31)$$

III. SIMULATION AND EXPERIMENTAL RESULTS

Figure 9 shows the simulation results, using Pspice simulation software, assuming $V_{AC} = 220V$, $L = 1 \text{ mh}$, $C_C = 22\mu\text{f}$, $I_{L,DC} = 10A$. To verify this control algorithm, we have made a small scale three-phase APF. The three-phase voltage reduces to 55 volts, with DC load $R_L = 40 \text{ ohm}$, $L = 1\text{mh}$, and the energy-storage capacitor $C_C = 22\mu\text{f}$. The capacitor reference voltage is set at 120V. The steady-state test results for $I_{DC} = 1.0 \text{ p.u.}$ are shown in Fig.10. The waveform of ch1 is the energy-storage capacitor voltage, ch2 is the utility current, ch3 is the converter output compensation current, and ch4 is the load current. The test results of transient response, using the advanced sampling technique, are shown in Fig. 11. The load current varies between $I_{DC} = 0.5 \text{ per unit (p.u.)}$ and $I_{DC} = 1.0 \text{ p.u.}$. When the load current increases from $I_{DC} = 0.5 \text{ p.u.}$ to $I_{DC} = 1.0 \text{ p.u.}$, the capacitor voltage drops down to V_{low} and the control circuit generates the sampling clock immediately to update the utility command current.

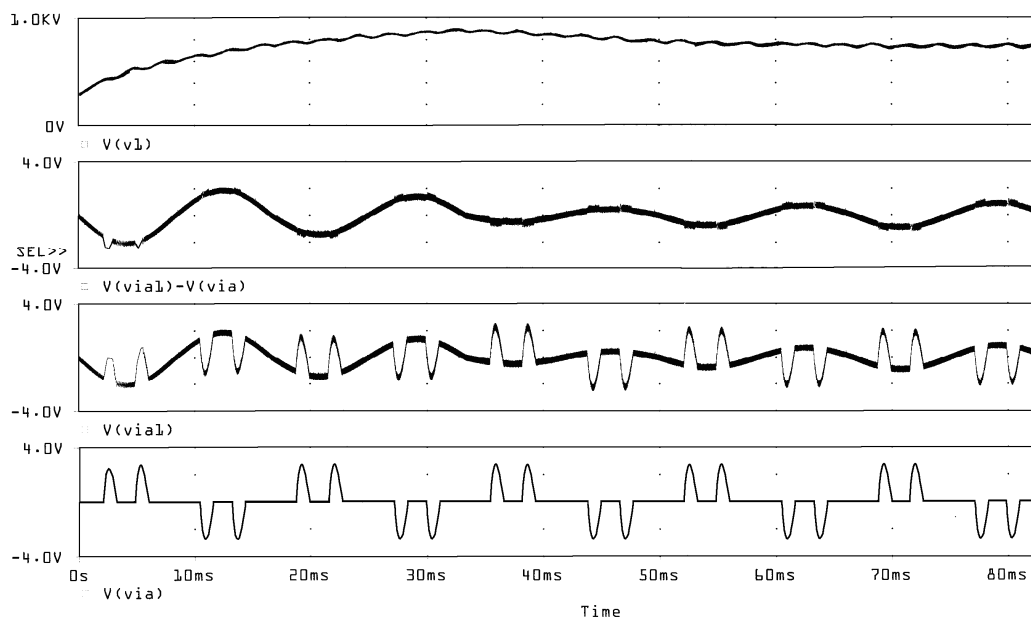


Fig. 9 The simulation results. Trace 1 is the capacitor voltage, trace 2 is line current, trace 3 is the compensation current and trace 4 is the load current

From the test results, we can see that the transient time is only one period. At the next new period, the system is already in steady-state. On the other hand, when the load current decreases from $I_{DC}=1.0$ p.u. to $I_{DC}=0.5$ p.u., the capacitor voltage is also kept in a reasonable range. Figure 12 shows the sampling clock of the proposed advanced sampling technique. From the test results, we can see that even we use a small size capacitor ($11\mu\text{f}/\text{amp}$) which may caused a large ripple; the compensation characteristics are still good enough.

IV. CONCLUSIONS

Due to the nonlinear load characteristics of much electronic equipment, the utility power system is polluted by harmonics and the power factor is decreased. In this paper, a new APF technique is proposed, using the sampling technique to simplify the calculation of the real fundamental component of the load current. In addition, the energy-balance concept in the energy-storage capacitor is used to simplify the design of the conventional APF capacitor voltage control circuit. The merits of this APF are: (1) Simplifying the calculation of the required utility source current $i_s(t)$, (2) A large ripple voltage can be tolerated in the energy-storage capacitor. Therefore, a smaller energy-storage capacitor is needed. (3) Only a proportional control method is applied in the controller design of the capacitor voltage. Hence the transient response is fast and good. The feasibility of the above scheme is verified by Pspice simulation and experimental results. The results demonstrate that the harmonics are suppressed and nearly unity power factor is obtained.

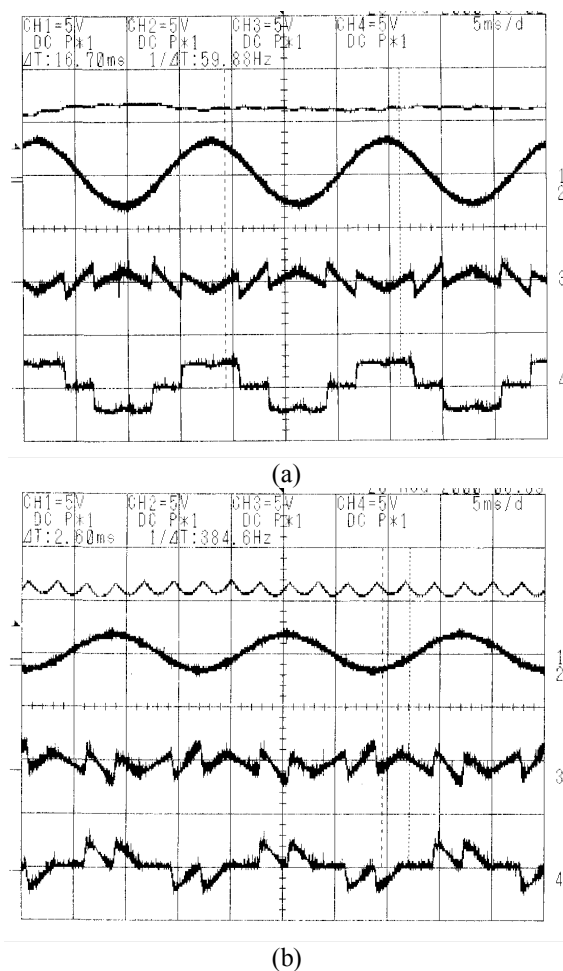
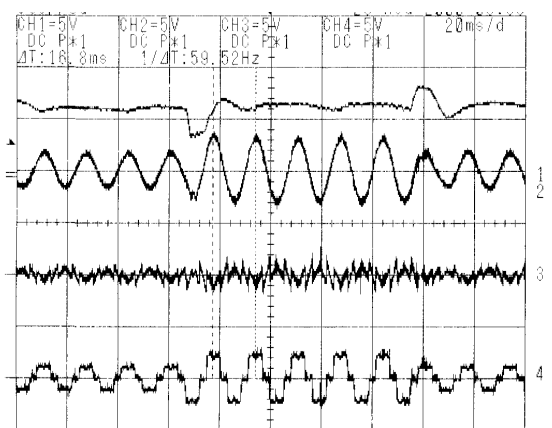


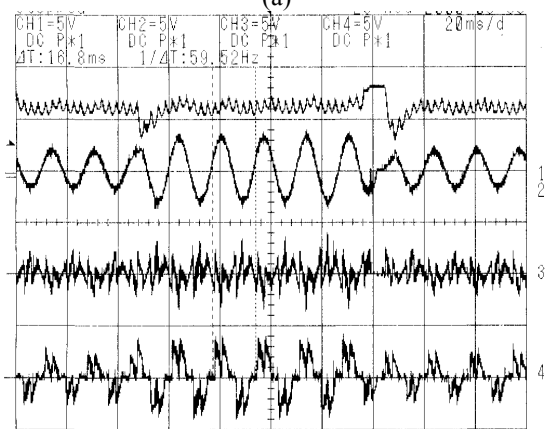
Fig. 10 The steady-state test results for load current varies between $I_{DC}=0.5$ p.u. and $I_{DC}=1.0$ p.u.. (a) R load. (b) R-C load

V. REFERENCES

- [1] F. M. P. Pamplona and B. A. Souza, "Harmonic passive filter planning in radial distribution systems using genetic algorithms," pp. 126-131, 2004.
- [2] G. Spiazzi, E. da Silver Martins, and J. A. Pomilio, "A simple line-frequency commutation cell improving power factor and voltage regulation of rectifiers with passive LC filter," 2001.
- [3] K. Chatterjee, G. Venkataramanan, M. Cabrera, and D. Loftus, "Unity power factor single phase AC line current conditioner," 2000.
- [4] H. L. Do and B. H. Kwon, "Single-stage line-coupled half-bridge ballast with unity power factor and ripple-free input current using a coupled inductor," *IEEE Transactions on Industrial Electronics*, vol. 50, pp. 1259-1266, 2003.
- [5] K. W. Siu, Y. S. Lee, and C. K. Tse, "Analysis and experimental evaluation of single-switch fast-response switching regulators with unity power factor," *IEEE Transactions on Industry Applications*, vol. 33, pp. 1260-1266, 1997.
- [6] M. Van der Berg, J. A. Ferreira, and W. Hofsaier, "A unity power factor low EMI battery charger for telecommunication applications," pp. 458-465.
- [7] C. Zhang, Q. Chen, Y. Zhao, D. Li, and Y. Xiong, "A Novel Active Power Filter for High-Voltage Power Distribution Systems Application," *IEEE Transactions on Power Delivery*, vol. 22, pp. 911-918, 2007.
- [8] G. W. Chang and C. M. Yeh, "Optimization-based strategy for shunt active power filter control under non-ideal supply voltages," *IEE Proceedings-Electric Power Applications*, vol. 152, pp. 182-190, 2005.
- [9] W. U. Jin-Chang and H. L. Jou, "Novel Circuit Topology for Three-Phase Active Power Filter," *IEEE Transactions on Power Delivery*, vol. 22, pp. 444-449, 2007.
- [10] H. L. Jou, J. C. Wu, Y. J. Chang, and Y. T. Feng, "A novel active power filter for harmonic suppression," *IEEE Transactions on Power Delivery*, vol. 20, pp. 1507-1513, 2005.
- [11] H. H. Kuo, S. N. Yeh, and J. C. Hwang, "Novel analytical model for design and implementation of three-phase active power filter controller," *IEE Proceedings-Electric Power Applications*, vol. 148, pp. 369-383, 2001.
- [12] B. Singh, B. N. Singh, A. Chandra, K. Al-Haddad, A. Pandey, and D. P. Kothari, "A review of three-phase improved power quality AC-DC converters," *IEEE Transactions on Industrial Electronics*, vol. 51, pp. 641-660, 2004.
- [13] K. P. Sozanski, "Shunt active power filter with improved dynamic performance," pp. 1995-1999, 2008.
- [14] X. Wei, K. Dai, X. Fang, P. Geng, F. Luo, and Y. Kang, "Parallel Control of Three-Phase Three-Wire Shunt Active Power Filters," 2006.
- [15] Y. C. Kuo, T. J. Liang, and J. F. Chen, "A high-efficiency single-phase three-wire photovoltaic energy conversion system," *IEEE Transactions on Industrial Electronics*, vol. 50, pp. 116-122, 2003.
- [16] Z. Chunyu, L. Yabin, and P. Yonglong, "A direct phase control scheme for unity power factor three-phase buck type rectifier based on SVPWM," 2006.
- [17] H. Do an and R. Akkaya, "A Simple Control Scheme for Single-Phase Shunt Active Power Filter with Fuzzy Logic Based DC Bus Voltage Controller," *Proceedings of the International MultiConference of Engineers and Computer Scientists*, vol. 2, 2009.
- [18] C. M. Liaw, T. H. Chen, T. C. Wang, G. J. Cho, C. M. Lee, and C. T. Wang, "Design and implementation of a single phase current-forced switching mode bilateral converter," *IEE Proceedings B [see also IEE Proceedings-Electric Power Applications] Electric Power Applications*, vol. 138, pp. 129-136, 1991.
- [19] L. Bowtell and A. Ahfok, "Comparison between unipolar and bipolar single phase grid connected inverters for PV applications," pp. 1-5, 2007.
- [20] T.-F. Lee, Y.-C. Hsiao, H.-Y. Wu, T.-L. Huang, F.-M. Fang, and M.-Y. Cho, "Optimization of reactive power compensation and voltage regulation using artificial immune algorithm for radial transmission networks," *Engineering Intelligent Systems*, vol. 15, pp. 107-113, 2007.



(a)



(b)

Fig. 11 The transient response test results for load current varies between $I_{DC}=0.5$ p.u. and $I_{DC}=1.0$ p.u.. (a) R load. (b) R-C load

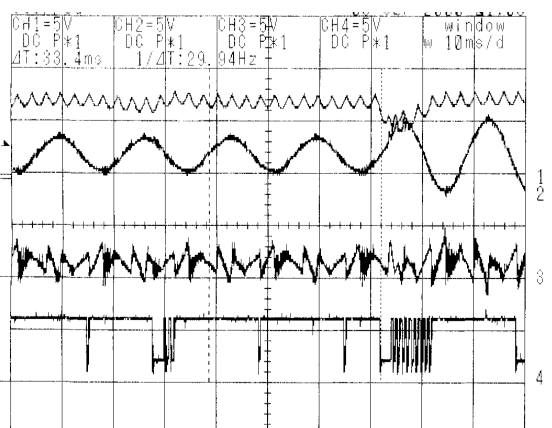


Fig. 12 The sampling clock of the proposed advanced sampling technique